

## Supporting Information for Lab on a Chip

### A continuous-flow microfluidic syringe filter for size-based cell sorting

Seungjeong Song, Miseok S. Kim, Jaeyeon Lee, and Sungyoung Choi\*

#### I. Experimental Section

##### Device fabrication

The microfluidic devices were fabricated by two-step photolithography and soft lithography. The first layer of SU-8 photoresist (Microchem Corp., MA) was patterned to define the main linear-channel structures; the second layer defined the patterns of slanted grooves on top of the channel structures in the first layer. After fabrication of the master mold, the mixture of PDMS and curing agent (Dow Corning, MI) in the ratio of 10:1 was poured on the mold and cured for 1 h on a hot plate at 70 °C. The cured PDMS was cut into individual devices and punched for inlet and outlet holes, and then the device was irreversibly sealed on a glass slide or PDMS slab after plasma activation for 40 s (Figure S5). The device was stored in an oven until used. The device comprises 240 ridges (40 ridges every step) with  $w = 550 \mu\text{m}$ ,  $h_g = 37 \mu\text{m}$ , and  $h_c = 119 \mu\text{m}$ , where  $w$  is the channel width,  $h_g$  is the height of the gap below the trenches, and  $h_c$  is the total channel height.

##### Material preparation

Device characterization was performed with polystyrene microparticles (Polysciences Inc., PA). The particles were suspended in 0.1% tween solution (Sigma-Aldrich Corp., MO) at a concentration of  $10^4$  to  $10^5$  particles  $\text{mL}^{-1}$ . MCF-7 cells and K562 cells were cultured in RPMI 1640 medium (Welgene, Korea) supplemented with 10% (v/v) heat-inactivated fetal bovine serum (Welgene, Korea), penicillin G ( $100 \text{ U mL}^{-1}$ ) and streptomycin ( $100 \mu\text{g mL}^{-1}$ ) at 37 °C in a humidified atmosphere containing 5%  $\text{CO}_2$ . For flow visualization of the cells, K562 cells were washed with DPBS (Welgene) and then stained with 10  $\mu\text{M}$  CFDA cell tracer (Invitrogen Inc., CA) at room temperature for 15 min. After staining, the cells were washed twice with DPBS. For cell

sorting, MCF-7 cells were centrifuged and resuspended in RPMI 1640 medium after passing through a 35- $\mu\text{m}$ -pore-size cell strainer (BD Biosciences, CA). For cell cycle analysis, 0.2 mL of cooled 70% ethanol was dropwise added to cell suspensions in 0.1 mL of DPBS and stored at 4°C for 2 hours. Subsequently, cells were pelleted by centrifugation and resuspended in 0.2 mg/ml RNase A solution (Sigma Aldrich, MO). After 60 min of incubation at 37°C, the cell suspensions were stained with 30  $\mu\text{g}/\text{ml}$  propidium iodide solution (Invitrogen) for 30 min and then flow cytometry was performed using Becton Dickinson Accuri C6 flow cytometer (BD Biosciences). The data was analyzed using a flow cytometry analysis software, FCS Express 4 Flow Cytometry (De Novo software, CA). For the purpose of analysis, 10,000 target cells were acquired after gating to eliminate cell aggregates and debris.

### **Experimental setup**

A syringe pump (KD Scientific Inc., MA) was used to produce a uniform flow rate over a range of 0.1 to 1.0 mL  $\text{min}^{-1}$  for device characterization. For sorting of microparticles and cells, they were injected into the device by manually pushing the plunger of 3-mL or 5-mL syringe. Flow trajectories of particles and cells were observed with a fluorescent microscope (Nikon, Japan).

### **Numerical simulation**

Flow simulations were performed with computational fluid dynamics software (CFD-ACE+; ESI, AL) to visualize pressure fields and velocity vector fields, and calculate the vorticity of the velocity fields. The velocity at the inlet was set to have a flow rate of 0.5 mL  $\text{min}^{-1}$ , while the pressure at the outlet was set to zero. Structured grids in the same dimensions with the channels of 1 step, 3 steps, and 6 steps were generated and simulated. No-slip boundary conditions were applied at the channel walls except the inlet and outlet.

## **II. Supplemental Discussion**

### **Application of continuous-flow microfluidic syringe filter to other systems**

To develop a continuous-flow microfluidic syringe filter as a new technique for cell separation, we chose a well-characterized and robust model, cell cycle synchronization of a cancer cell line

by size-based sorting to verify the principle. While we anticipate that the microfluidic syringe filter will be extended to other cell types, new applications will need to be developed on a case-by-case basis due to the need to tailor the geometric parameters to ensure cell sorting. In cases where cell populations are of similar size, non-target cell populations can be selectively labelled with microbeads to amplify their size and eliminate the size overlap with a target cell population.<sup>S1</sup> As a potential application of the syringe filter, we demonstrated the ability of the filter to remove cells and retrieve liquid medium which is a key unit laboratory operation for cell-based assays. We set  $h_g$  to 28  $\mu\text{m}$  to ensure complete focusing of K562 cells which have diameter of  $14.6 \pm 1.4 \mu\text{m}$  ( $n = 40$ ). Cells were injected at a volume throughput of  $0.8 \text{ mL min}^{-1}$  by manual operation that yielded a throughput of  $1.1 \times 10^5 \text{ cells min}^{-1}$ . The cells injected into the syringe filter were directed to the side outlets for cell rejection and no cells were found in hemocytometer cell counting of the sample collected at the liquid-medium outlet (Figure S6). These approaches could potentially enable the microfluidic syringe filter to be extended to other cell systems of practical interest.

### III. Supporting Figures

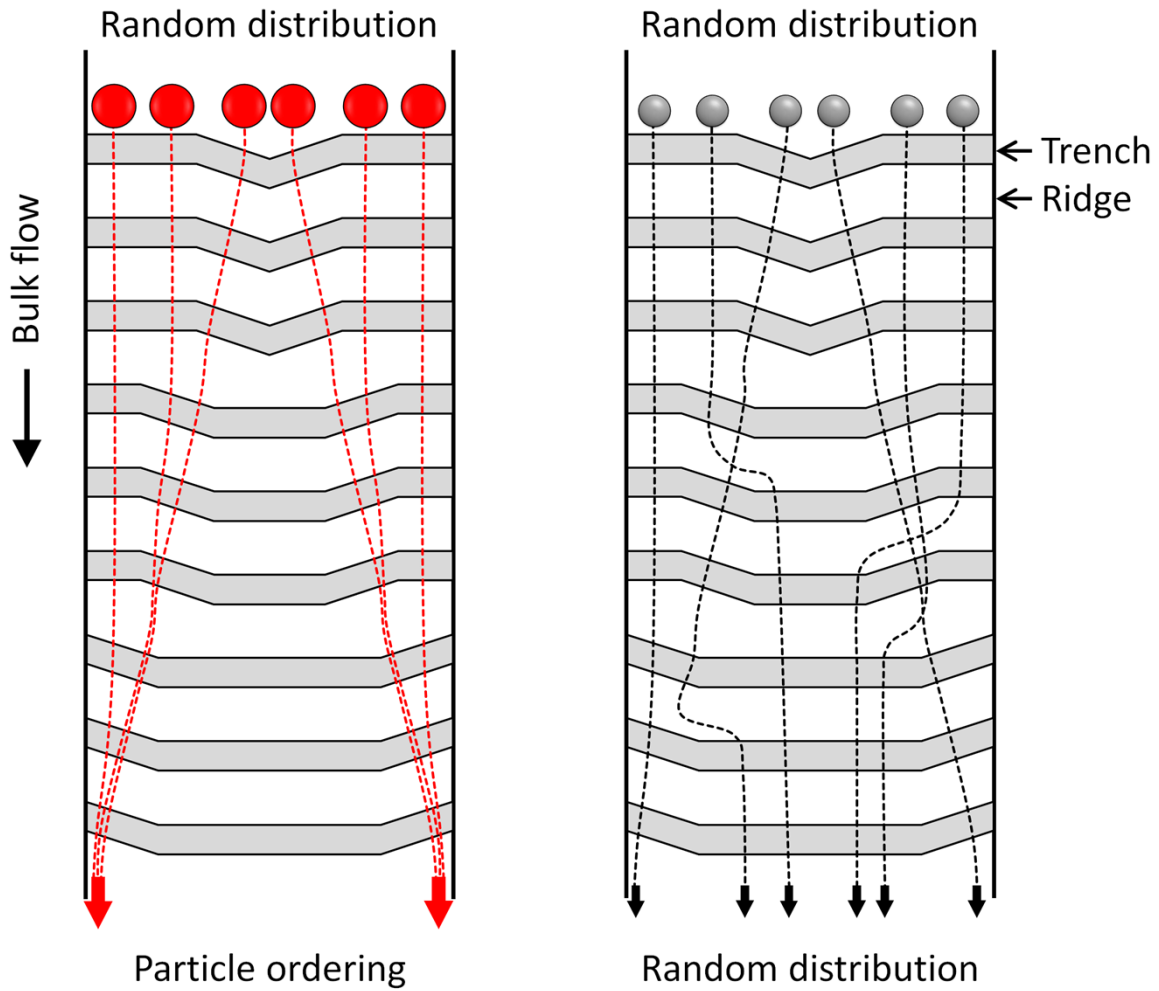


**FIG. S1.** Size dependence of particle ordering in the hydrophoresis device. Large particles satisfying  $h_g \leq 2d$  can be laterally migrated along the slanted geometry to the channel sides. Smaller particles not satisfying the criterion can follow similar paths as the streamlines, go up to the ridges, and move back and forth between the channel center and sidewalls.

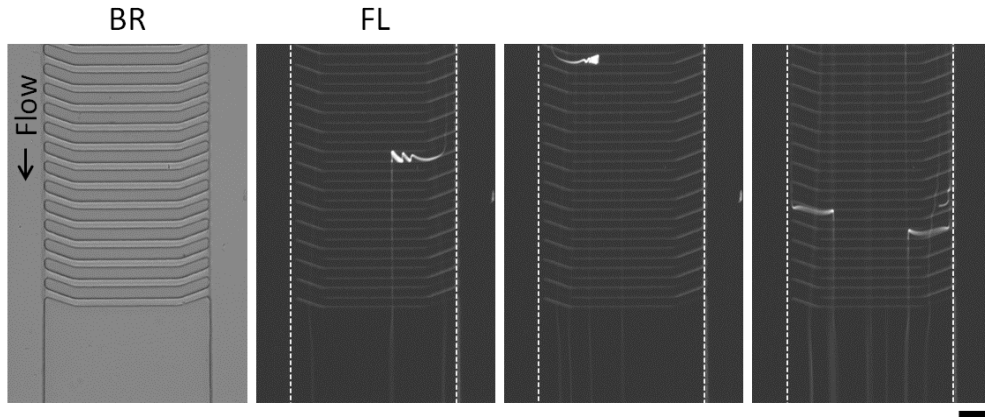


**FIG. S2.** Temporal trapping of 6.1  $\mu\text{m}$ -particles inside the ridges. When the small particles went up to the ridges, they were exposed to recirculating flows inside the ridges, moved in a helical manner toward the channel center, and finally came out of the ridges. BR and FL denote bright field and fluorescence, respectively. Scale bar = 100  $\mu\text{m}$ .

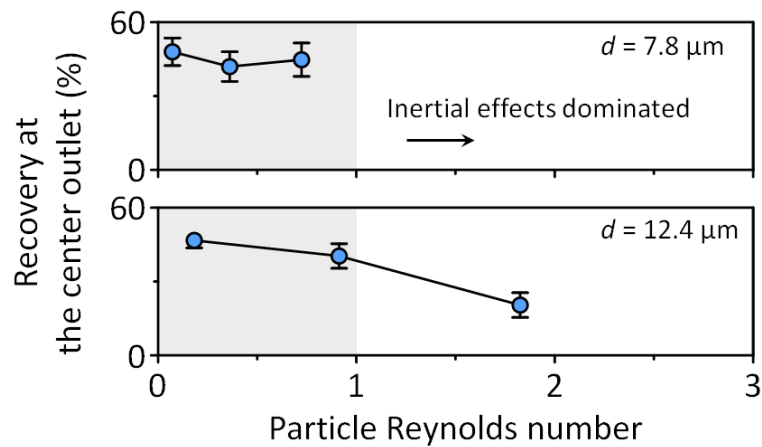


**FIG. S3.** Since the particle Reynolds number ( $Re_p$ ) of 7.8  $\mu\text{m}$ -particles is less than unity over a range of flow rates from 0.1 to 1.0  $\text{mL min}^{-1}$ , their recovery is not significantly affected by inertial effects. The ordering behavior of 12.4  $\mu\text{m}$ -particles starts to be affected at 0.5  $\text{mL min}^{-1}$  by inertial effects and becomes significant at 1.0  $\text{mL min}^{-1}$  due to increased  $Re_p$  over unity. The corresponding flow rate of each data point is 0.1, 0.5, and 1.0  $\text{mL min}^{-1}$  in an order of left to right.

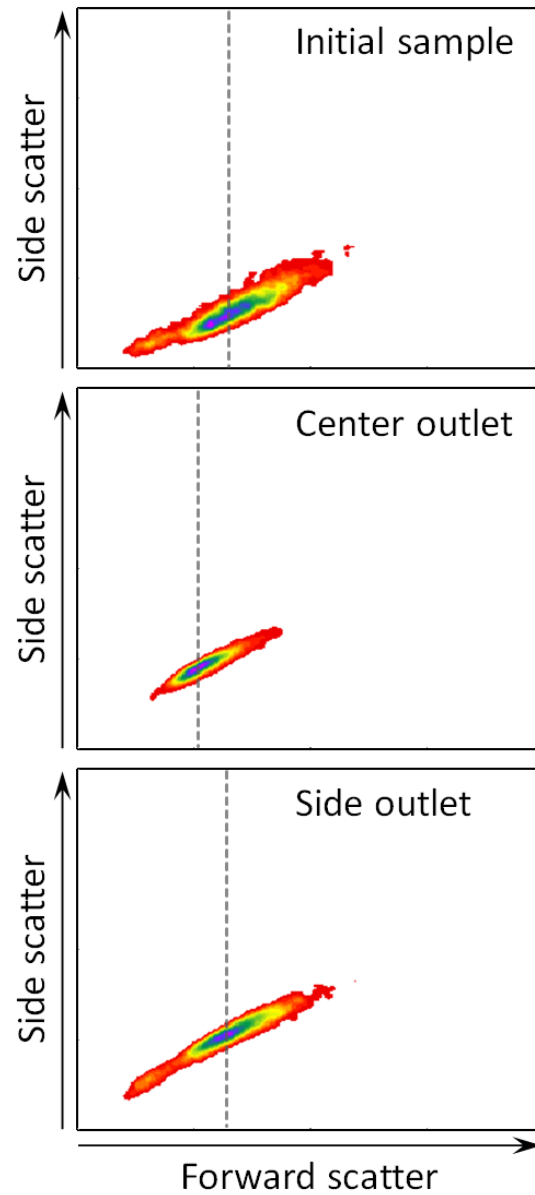


**FIG. S4.** Flow cytometry density plots showing the distribution of cells based on size (forward scatter) and internal complexity (side scatter) before and after separation. The cells collected at the center outlet show significant reduction in forward scatter intensity, a measure of cell size.

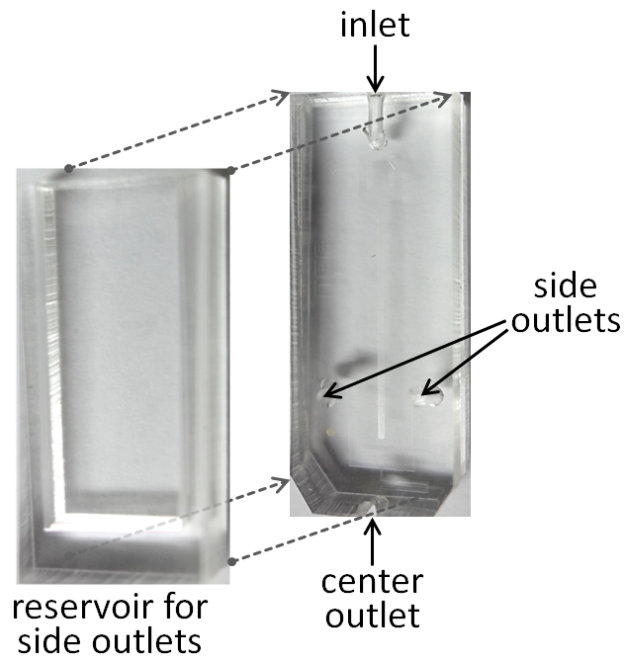


**FIG. S5.** The fabrication of the sorting device is completed by assembling a sorting channel composed of an inlet, a grooved channel, and three outlets and a reservoir for collecting particles/cells exiting from the side outlets.

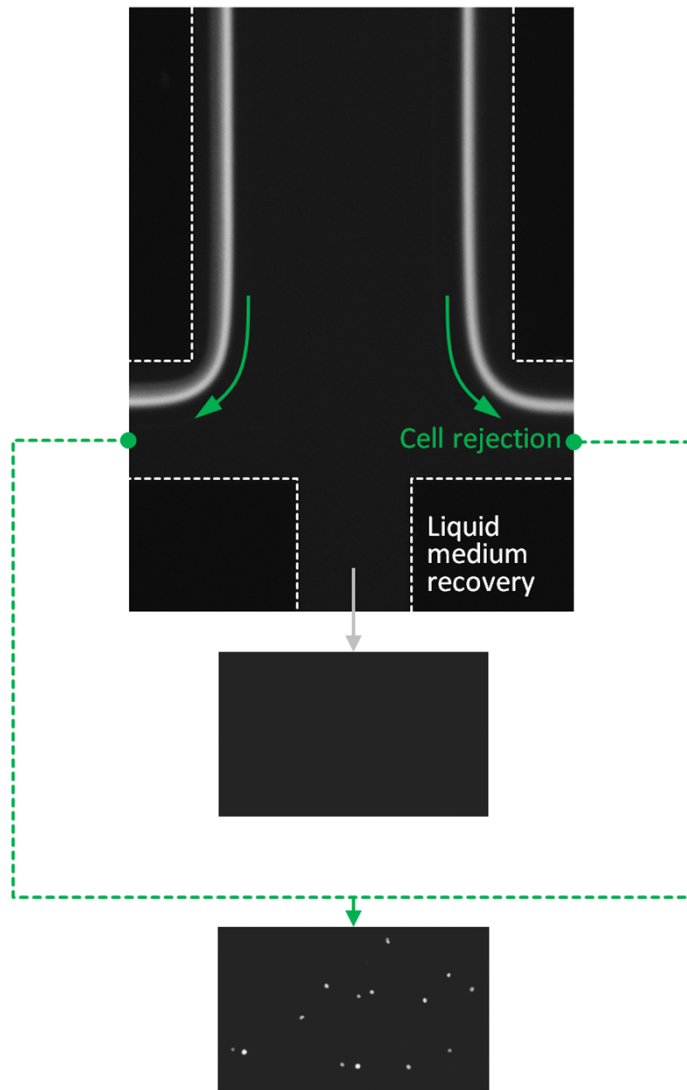


**FIG. S6.** Cell rejection and liquid-medium recovery using the microfluidic syringe filter. All the cells injected were directed to the side outlets, while cell-free liquid medium was collected at the center outlet.

#### **IV. Reference**

S1 J. H. Shin, M. G. Lee, S. Choi, and J.-K. Park, *RSC Adv.*, 2014, **4**, 39140.